SIMULATION OF HIGH-CYCLE FATIGUE-DRIVEN DELAMINATION IN CARBON/EPOXY LAMINATES USING COHESIVE ELEMENTS

K. Kiefer*, P. Robinson, S.T. Pinho

Department of Aeronautics, Imperial College London, London, UK
**k.kiefer09@imperial.ac.uk*

Keywords: delamination, high-cycle fatigue, cohesive elements, finite element modeling

Abstract
This paper discusses the implementation of a model for the high-cycle fatigue-driven delamination of a carbon/epoxy composite into the finite element software ABAQUS. The model was first tested using a non-FE technique which enabled an extensive investigation of its sensitivity and accuracy to be rapidly performed. It was then implemented as a user-defined element in the ABAQUS and will be used to predict the fatigue delamination of structural details for aerospace applications such as stiffener runouts.

1 Introduction
Delamination - the separation of two adjacent layers in a laminate - is an important failure mode to consider when designing components made from laminated carbon fibre reinforced polymer composites as it can reduce the structural stiffness and strength critically.
Delaminations in a structure are caused by high interlaminar stresses which occur for example at free edges, ply drops and corners. These interlaminar stresses can be caused by static loading and impact but also, as is the case of interest here, by low amplitude cyclic loading, where the number of load cycles may be in excess of one million.
There are two factors which make it very desirable to be able to model fatigue-driven delamination. Firstly, delamination often develops without any visible external sign and its detection requires using non-destructive testing methods such as ultrasound-based techniques to establish the magnitude of damage. A reliable fatigue model would increase the interval between inspections. Secondly, computer simulations with many loading cycles are cheaper and take significantly less time than an experimental fatigue test where the whole lifetime of the structural component is simulated. It is therefore of considerable interest to be able to model delamination numerically so as to understand how delamination might develop in a particular structural design and how the design could be improved to be less susceptible to delamination.
A common modeling strategy in finite element (FE) models is to insert cohesive elements [1] where delaminations are thought likely to occur. Cohesive elements have been employed extensively for delamination growth under quasi-static loading and more recently have been adapted to also model fatigue-driven delamination.
In this paper a damage model that has been evaluated previously has been implemented into a cohesive user element (UEL) in ABAQUS which is then to be used to simulate stiffener runouts.

2 Damage models

2.1 Paris law

The model is validated against a modification of the Paris law [2], a widely used curve fitting model, where the modification consists of using the strain energy release rate range ΔG rather than the stress intensity factor range ΔK. Fatigue crack growth is characterized by three zones as shown in Figure 1. The model has been used to simulate crack growth in the middle zone (zone 2), where the Paris power law applies

$$\frac{da}{dN} = C\left(\Delta G\right)^m . \tag{2.1}$$

In this equation a is the crack length, N the number of cycles, and C and m are material properties which have to be determined experimentally for a given material.

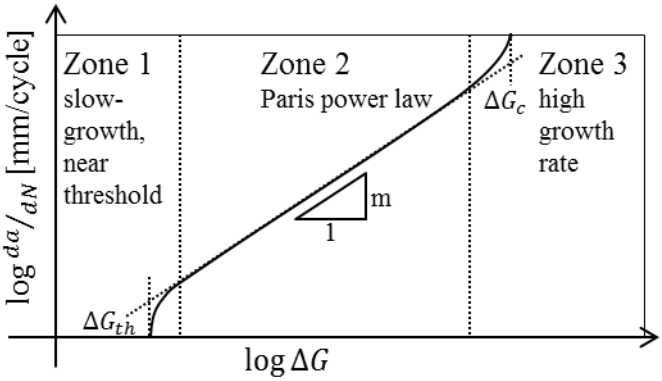

Figure 1. *log-log* plot of fatigue crack growth rate vs. strain energy release rate

2.2 Cohesive zone model

The cohesive element is a zero-thickness finite element with initially coinciding top and the bottom surfaces representing the crack faces. It is based on the cohesive zone model introduced by Dugdale and Barenblatt [3,4], which assumes that there is a softened zone at the tip of a crack where stresses are not yet zero and are dependent on the relative displacement between the two crack faces. This section deals with this stress-displacement relationship also called the constitutive law, which in the case of fatigue-driven delamination is made dependent on the number of cycles.

Since it would be too computationally expensive to model individual cycles when dealing with high-cycle fatigue, the fatigue model outlined below is a cycle-jump model, where a certain number of cycles are simulated blockwise each step. This means also that numerically applied loads and numerically computed displacements are envelopes of the cyclic curves (see figure 1).

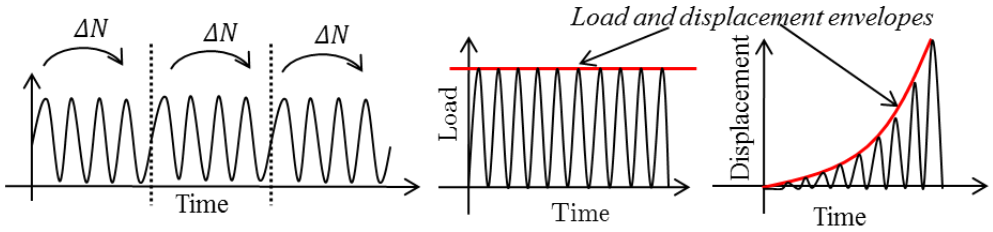

Figure 2. Cycle Jump strategy (left), load and displacement envelopes (centre and right)

2.3 Fatigue degradation strategy

The fatigue degradation strategy that is used in this paper has been originally developed by Robinson et.al. [5]. It is explained here for mode I. The static constitutive relationship used is the bilinear law shown in figure 3 for mode I and mode II.

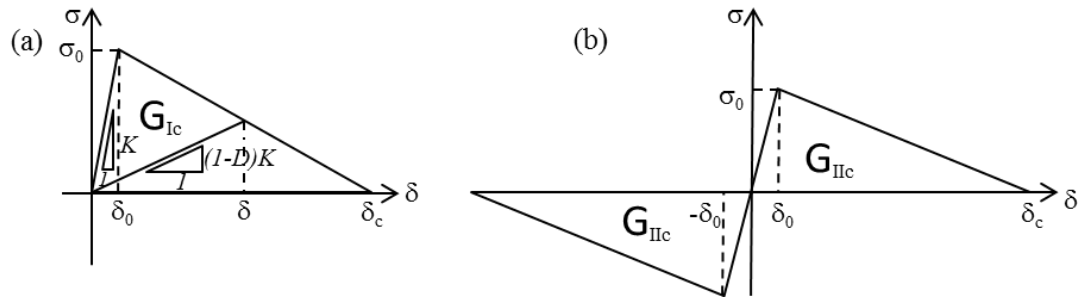

Figure 3. Bilinear constitutive law in (a) mode I and (b) mode II

The traction with respect to the damage is expressed as follows

$$\sigma = (1 - D) K \delta, \tag{2.2}$$

where the damage is divided into a static and a fatigue part, D_s and D_f respectively for which $D=D_s+D_f$. The static damage can be written in terms of the displacement as

$$D_s(\delta) = \frac{\delta_c}{\delta} \frac{\delta - \delta_0}{\delta_c - \delta_0} \quad for \quad \delta_0 < \delta \leq \delta_c, \tag{2.3}$$

with $D_s=0$ when δ is below δ_0 and $D_s=1$ otherwise. The change in static damage between N cycles and $N+\Delta N$ can then be computed from the respective displacements and equation (2.3) as

$$\Delta D_s = \frac{\delta_0 \delta_c}{\delta_c - \delta_0} \left(\frac{1}{\delta(N)} - \frac{1}{\delta(N + \Delta N)} \right). \tag{2.4}$$

The fatigue damage is introduced in the following way, which was first proposed by Peerlings [6] following a modified version by Paas [7]

$$\dot{D}_f = \frac{\partial D_f}{\partial t} = A e^{\lambda D} \left(\frac{\delta}{\delta_c} \right)^{\beta} \frac{\dot{\delta}(t)}{\delta_c} \tag{2.5}$$

where β, λ, and A are parameters which have to be determined so that the resulting crack growth is in agreement with the experimentally determined Paris law and δ/δ_c is a normalized displacement. Using this damage rate, fatigue damage can occur when the initial damage is zero and thus a crack can grow even in an initially undamaged interface. The derivation of the damage growth rate per cycle given below is explained in detail in [5].
The fatigue damage after a number of cycles ΔN has elapsed can be found by integrating the fatigue damage rate over the respective number of cycles. This integration is performed numerically. A constant μ with $0 \leq \mu \leq 1$ is found, so that

$$\Delta D_f = \int_N^{N+\Delta N} \frac{A}{1+\beta} e^{\lambda D(N)} \left(\frac{\delta(N)}{\delta_c} \right)^{1+\beta} dN = \Delta N \frac{\partial D_f(D_\mu, \delta_\mu)}{\partial N}, \tag{2.6}$$

$$\begin{aligned} D_\mu &= (1-\mu) D(N) + \mu D(N+\Delta N) \\ \delta_\mu &= (1-\mu)\delta(N) + \mu\delta(N+\Delta N). \end{aligned} \tag{2.7}$$

In this paper a value for μ of 0.7 was used. Combining equations (2.4) and (2.6), the damage evolution with respect to a cycle jump ΔN can thus be expressed as

$$D(N+\Delta N) = D(N) + \Delta D_s + \Delta D_f \tag{2.8}$$

This implicit formulation for $D(N+\Delta N)$ is approximated using a Newton-Raphson algorithm.

2.4 Evaluation with simple cylinder model

2.4.1 Cylinder model

For the investigation of fatigue damage laws in mode I, a mathematical non-FE model was used [8]. This allows for a very fast assessment of potential fatigue degradation strategies compared to a full finite element analysis. The model, referred to as the cylinder model, which is shown in figure 4, consists of two zero-thickness layers of a fixed width *W*. The bottom layer is attached to the ground and the top one to a cylinder of sufficiently large radius *R*, to which an external moment M_a is applied.

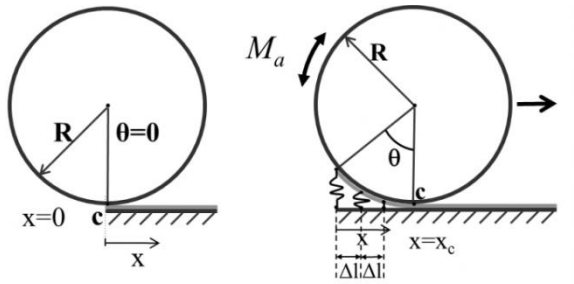

Figure 4. Cylinder model showing extended springs, element spacing *Δl* and contact point xc

The interface is simulated by initially unstressed equidistant springs, which fulfill the same role as a cohesive element in finite element modeling (FEM). The springs are associated with a constitutive law and a degradation strategy, which determine the stress in terms of the number of cycles passed and the displacement. These individual spring stresses are then used to determine a resisting moment contribution about the contact point *c* (see figure), which is found by multiplying the cohesive stress with the interface area represented by the spring and the distance from the contact point. The total resisting moment is then determined by summing up the moment contributions of all the individual springs. An equilibrium angle θ can then be found at which the external moment is equal in magnitude to the resisting moment.

With a relatively simple energy balance the applied energy release rate G_a can be calculated from the external moment, which is required as an input for the Paris law. The work done by the external moment as the cylinder rotates by $\Delta\theta$, causing the contact point *c* to move by a distance of Δx has to be equal to the energy consumed in the interface separation

$$M_a \Delta\theta = \Delta x G_a W. \tag{2.9}$$

The change in angle $\Delta\theta$ can be related to the arc-length Δx through simple trigonometry and therefore

$$M_a \frac{\Delta x}{R} = \Delta x G_a W \Rightarrow M_a = G_a W R \tag{2.10}$$

2.4.2 Results

The fatigue degradation strategy stated above and a second one introduced by Turon et. al [9] were examined and compared with each other previously using the cylinder model [10].
For this comparison sensitivity studies were undertaken for both strategies in order to determine the relative errors in growth rates with respect to two important parameters. One of them is the element size Δl. The strategies are more accurate for small element sizes, but having very small elements increases the simulation runtime drastically and it is therefore desirable to have a model that is tolerant to an increase in element size.
The other parameter tested was the number of cycles per step ΔN. This also has a very great influence on the runtime of the model since for every fatigue step of the finite element model, a new equilibrium has to be found. The Peerling fatigue strategy produced smaller errors for larger element sizes and cycle jumps and was therefore chosen to be implemented into the cohesive element.

3 Implementation in ABAQUS

The three-dimensional, eight-noded cohesive element is shown in figure 5 in its initial unstressed configuration, where top and bottom surface coincide. The displacement field is interpolated with linear shape functions. A detailed derivation can be found in [11] and [12].
Following the advice of Schellekens and de Borst [13] who found that Gauss integration can cause oscillations in the calculated traction due to the high initial stiffness of the constitutive law, which magnifies initial oscillations in the displacement, a Newton-Cotes integration scheme was applied at first. However this caused spurious uneven growth along the crack front, an effect which has been described by Davila et.al [14]. In order to be able to analyse single-element-wide FE models of a mode I double cantilever beam (DCB), a Gaussian integration scheme has therefore been used and the initial stiffness has been reduced from 10^6 N/mm^3 to 10^5 N/mm^3.
The cohesive element is implemented in Fortran 90 as a user subroutine (UEL) into ABAQUS 6.10. The user subroutine is called once per increment for every user element and passes the stiffness matrix and force vector contribution back to the finite element software.

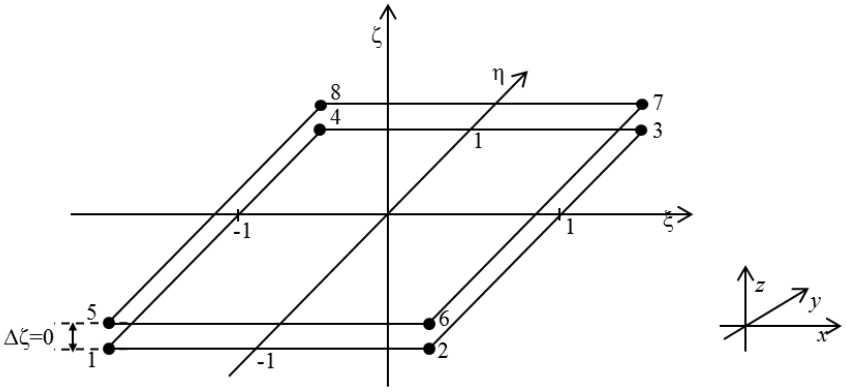

Figure 5. Initial configuration of cohesive element

The fatigue damage accumulation is incorporated by using a predefined field, which tracks the number of cycles. This information is passed to the user subroutine which then computes the accumulated damage accordingly. The constitutive response for static and fatigue delamination is currently implemented for mode I.

4 Initial Results

The cohesive element was first tested using a double cantilever beam (DCB) model with a pre-crack and fixed at the end as shown in figure 6. The beam was modeled with an orthotropic material.

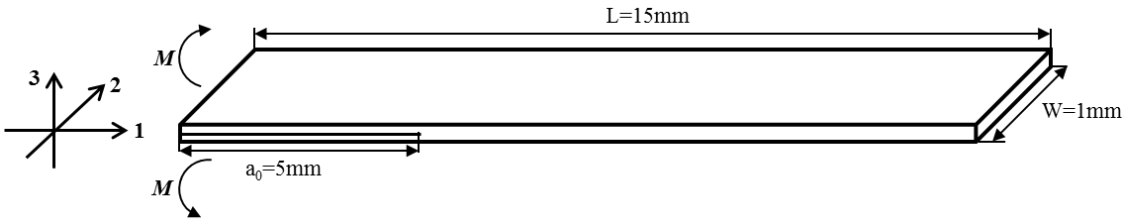

Figure 6. DCB model

The material properties and interface properties [5] as well as the Peerling degradation parameters used are shown in table 1.

Material properties	Interface properties	Peerling parameters
E_{11} = 120 GPa	σ_0= 30 MPa	β=2.0
E_{22} = E_{33}=10.5 GPa	G_{Ic}=0.268 N/mm	λ=0.5
G_{12} = G_{13} = 5.25 GPa	K= 10^5 N/mm^3	A=7.5e-04
G_{23} = 3.48 GPa		
ν_{12} = ν_{13} = 0.3		
ν_{23} = 0.51		

Table 1. Material properties, interface properties and Peerling parameters

A layer of cohesive element was placed between the arms to simulate the gradual delamination. In order to keep the energy release rate at the crack tip constant, a constant bending moment was applied to both arms. The energy release rate can then be computed as follows [15]

$$G_I = \frac{M^2}{E_{11} W I} \tag{2.11}$$

In a first step, the moment was ramped up to a fixed value. In the second step, a predefined field was applied to simulate the passing of cycles, while the moment was kept constant at the same value as in the first step. The crack growth rate was then recorded with respect to the number of cycles. This growth rate is subsequently compared to experimental data taken from [16]. The results, which are shown in figure 7 demonstrate good agreement with the experiment.

.

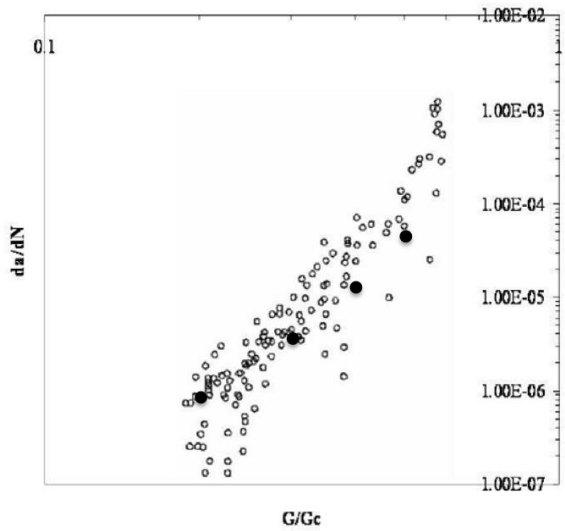

Figure 7. Mode I Paris law. ○ experimental ● numerical.

5 Further Work

In order to predict the delamination of stiffener runouts such as the one shown in figure 8 [17] which fail in pure mode II the model above has to be adapted.

The cylinder model described above allows for the examination of fatigue degradation strategies in mode I only. However, it is possible to use analogous fatigue degradation strategies for shear using the mode II constitutive law shown in figure 3. Since the numerical algorithm is essentially the same, the sensitivity studies undertaken with the cylinder model are transferable to the mode II case.

The mode I cohesive user element will be adapted to allow for pure mode I and mode II delamination. The next step is then to extend this to mixed-mode delamination.

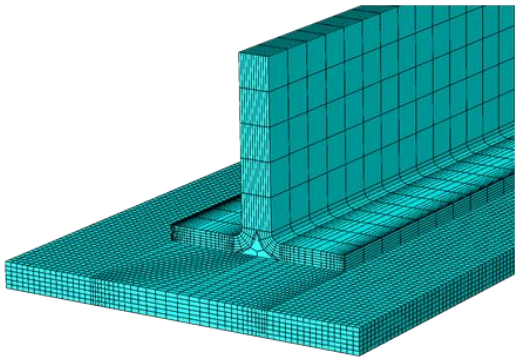

Figure 8. Finite element model of stiffener runout [17]

6 Conclusions

A cohesive user element for the simulation of fatigue-driven delamination growth was presented. A previously examined fatigue degradation strategy was incorporated into a user subroutine UEL in ABAQUS. The implementation was realised in Fortran 90. The cohesive user element was successfully tested for static delamination and mode I high-cycle-fatigue delamination. It will now be adapted to be able to model mode II delamination.

Acknowledgements

This research has received funding from the European Community's Seventh Framework Program FP7/2007-2013 under grant agreement n°213371 (www.maaximus.eu).

References

[1] Alfano G., Chrisfield M.A. Finite element interface models for delamination analysis of laminated composites. *International Journal for Numerical Methods in Engineering*, **50**, pp. 1701-1736 (2001)

[2] Schoen J. A model of fatigue delamination in composites. *Composites Science and Technology*, **60**, pp. 553-558 (1999)

[3] Barenblatt G.I. The mathematical theory of equilibrium cracks in brittle fracture. *Advances in Applied Mechanics*, **7**, pp. 55-129 (1962)

[4] Dugdale D.S. Yielding of steel sheets containing slits. *Journal of the Mechanics and Physics of Solids*, **8**, pp. 100-104 (1960)

[5] Robinson P., Galvanetto U., Tumino, D., Bellucci G., Violeau D. Numerical simulation of fatigue-driven delamination using interface elements, *International Journal for Numerical Methods in Engineering*, **63**, pp. 1824-1848 (2005)

[6] Peerlings R.H.J, Brekelmans W.A.M., de Borst R., Geers M.G.D. Gradient-enhanced damage modeling of high-cyclic fatigue. *International Journal for Numerical Methods in Engineering*, **49**, pp.1547-1569, (2000)

[7] Paas M.H.J.W., Schreurs P.J.G., Brekelmans W.A.M. A continuum approach to brittle and fatigue damage: theory and numerical procedures. *International Journal of Solids and Strutures*, **30**, pp.579-599 (1993)

[8] Galvanetto U., Robinson P., Cerioni A., Lopez Armas C. A Simple Model for the Evaluation of Constitutive Laws for the Computer Simulation of Fatigue-Driven Delamination in Composite Materials. *SDHM: Structural Durability & Health Monitoring*, **5**, pp. 161-190 (2009)

[9] Turon A., Costa J., Camanho P.P., Davila C.G. Simulation of delamination in composites under high-cycle fatigue. *Composites Part A*, **38**, pp. 2270-2282 (2007)

[10] Kiefer. K, Robinson P., Pinho S.T. *Comparison of models for the simulation of fatigue-driven delamination using cohesive elements* in "Proceedings of the *18th International Conference on Composite Materials*" , Jeju Island, South Korea (2011)

[11] Feih S. *Development of a user element in ABAQUS for modeling of cohesive laws in composite structures.* Riso National Laboratory, Roskilde, Denmark (2005)

[12] Turon Travesa A. *Simulation of delamination in composites under quasi-static and fatigue loading using cohesive zone models*. PhD thesis. University of Girona, Spain (2006)

[13] Schellekens, J.C.J. and de Borst, R. On the numerical integration of interface elements. *International Journal for Numerical Methods in Engineering*, **36**, pp. 43-66 (1993)

[14] Davila C.G., Camanho P.P., Turon A. Cohesive elements for shells. *NASA/TP-2007-214869* (2007)

[15] Mi Y., Crisfield M.A. Analytical derivation of load/displacement relationship for the DCB and MMB and proof of the FEA formulation. *IC-AERO Report 97-02*, ISSN 0308-7247.

[16] Greenhalgh E.S., Asp L.E., Sjoergen A. Delamination growth and thresholds in a carbon/epoxy composite under fatigue loading. *Journal of Composites Technology andResearch*, **23**, pp 55-68 (2001)

[17] Psarras S. *Investigating failure in composite stiffener run-outs*. PhD thesis. Imperial College London, UK (2012)